

## **Influence of Cr substitution on the reversibility of the magnetocaloric effect in Ni-Cr-Mn-In Heusler alloys**

Salazar Mejia, C.; Devi, P.; Singh, S.; Felser, C.; Wosnitza, J.;

Originally published:

October 2021

**Physical Review Materials 5(2021), 104406**

DOI: <https://doi.org/10.1103/PhysRevMaterials.5.104406>

Perma-Link to Publication Repository of HZDR:

<https://www.hzdr.de/publications/Publ-33244>

Release of the secondary publication  
on the basis of the German Copyright Law § 38 Section 4.

# Influence of Cr substitution on the reversibility of the magnetocaloric effect in Ni-Cr-Mn-In Heusler alloys

C. Salazar-Mejía,<sup>1,\*</sup> P. Devi,<sup>2,3,4</sup> S. Singh,<sup>2,5</sup> C. Felser,<sup>2</sup> and J. Wosnitzer<sup>1,6</sup>

<sup>1</sup>*Hochfeld-Magnetlabor Dresden (HLD-EMFL) and Würzburg-Dresden Cluster of Excellence ct.qmat, Helmholtz-Zentrum Dresden-Rossendorf, 01328 Dresden, Germany*

<sup>2</sup>*Max Planck Institute for Chemical Physics of Solids, 01187 Dresden, Germany*

<sup>3</sup>*Center for Quantum Nanoscience, Institute for Basic Science (IBS), Seoul 03760, Republic of Korea*

<sup>4</sup>*Ewha Womans University, Seoul 03760, Republic of Korea*

<sup>5</sup>*School of Materials Science and Technology, Indian Institute of Technology (BHU), Varanasi-221005, India*

<sup>6</sup>*Institut für Festkörper- und Materialphysik, TU Dresden, 01062 Dresden, Germany.*

(Dated: August 11, 2021)

We present the effect of substitution-induced pressure on the reversibility of the magnetocaloric effect (MCE) in  $\text{Ni}_2\text{Cr}_x\text{Mn}_{1.4-x}\text{In}_{0.6}$  ( $x = 0.1, 0.2, 0.3$ ) alloys, through characterization in pulsed magnetic fields. We measured the adiabatic temperature change,  $\Delta T_{ad}$ , directly during applied magnetic field pulses of 2 and 6 T. We paid special attention to the reversibility of  $\Delta T_{ad}$ . The substitution of Mn by Cr in the  $\text{Ni}_2\text{Mn}_{1.4}\text{In}_{0.6}$  leads to a negative pressure, as evidence by the increase of the lattice parameters, which shifts the martensitic transition towards lower temperatures and enhances the ferromagnetism of the martensite phase. A large value of  $\Delta T_{ad} = -7$  K at  $T = 270$  K is recorded on the  $x = 0.1$  sample for a field change of 6 T. We discuss the reversibility of the MCE in these alloys in terms of the Clausius-Clapeyron equation.

## I. INTRODUCTION

Ni-Mn-based shape-memory Heusler alloys are well known for their fascinating multifunctional properties such as giant magnetocaloric effect (MCE) [1, 2], giant barocaloric effect [3], field-induced shape-memory effect [4] and magnetic superelasticity [5]. These properties are closely related to the first-order martensitic transition appearing in these alloys. The MCE manifests itself as a change in the temperature of a material by applying magnetic field and can be quantified in terms of isothermal entropy and adiabatic temperature change [1, 5–7]. Heusler alloys exhibit large magnetocaloric effects, however, missing reversibility is an issue that has been extensively studied and discussed [7–13].

Our previous reports show a detailed study of the MCE in pulsed magnetic fields for the shape-memory Heusler alloy  $\text{Ni}_2\text{Mn}_{1.4}\text{In}_{0.6}$  [8]. This alloy exhibits a conventional MCE of  $\Delta T_{ad} = 5$  K around 315 K (the Curie temperature) and a large inverse MCE of  $\Delta T_{ad} = -7$  K at 250 K (martensitic transition) under a magnetic field change of 6 T [8]. However, the inverse MCE is irreversible. Recently, we have shown that reversible MCEs can be obtained in Ni-Mn-based shape-memory Heusler alloys as a result of improving the compatibility between the austenite and martensite crystal structures [7, 9]. We have also reported on the effect of externally applied pressure on the reversibility of the MCE in Ni-Cu-Mn-In Heusler alloys [14]. Another strategy to improve the reversibility of the MCE in the Ni-Mn-based family of alloys is a tailored substitution of the transition elements and, in this way, reducing or increasing the chemically induced-pressure without avoiding the first-order phase transition that leads to the large inverse MCE.

Predictions from first-principles, Monte Carlo and ab-initio

calculations show that Cr substitution in Ni-Mn-In-based Heusler alloys could lead to a large inverse MCE due to a large magnetization jump at the martensitic transition. This is due to the appearance of a paramagnetic or antiferromagnetic gap at temperatures below the structural transformation [15, 16]. Ab-initio calculations reported in Ref. 16 indicate the  $\text{Ni}_2\text{Cr}_{0.25}\text{Mn}_{1.25}\text{In}_{0.5}$  as the most suitable composition in Ni-Cr-Mn-In-based alloys for application in magnetic refrigeration. It is predicted that the martensite phase on this alloy is ferrimagnetic while the austenite is ferromagnetic and consequently, a large magnetization jump should be observed at the structural transition from martensite to austenite [16]. Different attempts to substitute Cr in the Ni-Mn-In alloys have been reported in literature [17–20]. Controversial results have been reported, for instance, the unusual effect of Cr to increase the martensitic transition temperature despite the concomitant decrease of the valence electron concentration per atom,  $e/a$  [18, 20]. Sanchez-Alarcos et al. [21] have pointed out a very low solubility of Cr in Ni-Mn-In, which leads to the appearance of a Cr-rich second phase, even for quite low Cr concentrations. It has been also reported that substitution of Cr for Ni in  $\text{Ni}_{50-x}\text{Cr}_x\text{Mn}_{37}\text{In}_{13}$  enhances the MCE [17]. Thus, the effect of Cr doping in the Ni-Mn-In-based alloys, in terms of composition stability, phase transition behavior and MCE is not yet clear from the experimental point of view. Moreover, a direct measurement of adiabatic temperature change and its reversibility, which is important for the technological application of these alloys, has not been addressed in the literature.

In the present manuscript, we have successfully prepared single-phase shape-memory Heusler alloys of the series  $\text{Ni}_2\text{Cr}_x\text{Mn}_{1.4-x}\text{In}_{0.6}$ , with  $x = 0.1, 0.2$ , and  $0.3$ . We have investigated the magnetic and magnetocaloric properties in the view of possible applications. Substitution of the low atomic number transition element Cr for Mn tunes the structural and ferromagnetic transition towards lower temperatures. All samples show a structural transition in the temperature range

\* c.salazar-mejia@hzdr.de

between 200 and 300 K, below the Curie temperature,  $T_C$ . We have characterized the magnetocaloric effect (specifically, the adiabatic temperature change  $\Delta T_{ad}$ ) due to the martensitic magnetostructural transformation in these alloys, under applied magnetic field pulses of 2 and 6 T. All of these shape-memory Heusler alloys exhibit a large inverse MCE (temperature decrease under field application) due to the field-induced martensitic transition and a conventional MCE (temperature increase under field application) associated with the ferromagnetic transition.

## II. EXPERIMENTAL DETAILS

We prepared polycrystalline ingots of  $\text{Ni}_2\text{Cr}_x\text{Mn}_{1.4-x}\text{In}_{0.6}$  ( $x = 0.1, 0.2, \text{ and } 0.3$ ) by induction melting from high-purity commercially available elements of Ni, Cr, Mn, and In in an Ar atmosphere with an overall mass loss of less than 0.02 wt.%. A two-step process was employed for each sample. First, a pre-melt of Ni-Cr was prepared. According to the phase diagram, Ni and Cr react very well with each other and form a stable phase. In the next step, when the pre-melt is heated, it absorbs the Mn and In pieces that we added to the melt. As a result, after the Mn and In are absorbed, evaporation of the complete phase, not the single elements, takes place. All samples were melted four times on each side to ensure homogeneity. The melted ingots were then annealed at 900° C for three days and subsequently quenched into an ice water mixture.

We performed structural characterization at room temperature (RT) with powder X-ray diffraction (XRD) using a Huber G670 camera (Guinier technique,  $\lambda = 1.54056 \text{ \AA}$ ,  $\text{Cu-}K\alpha$  radiation). Prior to doing XRD, all samples were ground into powder and annealed at 700° C, which reduces the stress generated during grinding [14, 22]. Scanning electron microscopy (SEM) and Energy dispersive X-ray (EDX) were used to study the composition. Prior to SEM and EDX analyzes, small pieces were cut from the samples with a diamond saw. To prepare a smooth surface, the pieces were embedded in epoxy-resin blocks and polished.

We carried out magnetization measurements in a Physical Property Measurement System (PPMS, Quantum Design). Direct measurements of  $\Delta T_{ad}$  were performed in a home-built experimental setup in pulsed magnetic fields at the Dresden High Magnetic Field Laboratory (HLD). Short pulse durations (20-50 ms) allow for adiabatic conditions, making possible to measure  $\Delta T_{ad}$  without heat losses [8].

## III. RESULTS AND DISCUSSION

The observed and calculated ( $L2_1$  cubic structure, space group  $Fm\bar{3}m$ ) XRD patterns at RT for all samples are presented in Fig. 1. The observed Bragg reflections (for all samples) are accounted very well by the cubic  $L2_1$  crystal structure, which reveals the phase purity of the samples. The refined lattice parameters are  $a = 6.005 \text{ \AA}$  for  $x = 0.1$ ,  $a = 6.012 \text{ \AA}$  for  $x = 0.2$ , and  $a = 6.037 \text{ \AA}$  for  $x = 0.3$ , which

TABLE I. Element concentration determined by EDX at four different spots on the samples, as indicated in the insets of Fig. 1.

Alloy	Spot	Ni (at%)	Mn (at%)	Cr (at%)	In (at%)
0.1	1	47.55	31.97	1.98	18.49
	2	49.99	30.44	2.19	17.38
	3	49.78	30.74	2.50	16.99
	4	48.94	30.05	2.55	18.45
0.2	1	48.99	29.57	5.65	15.80
	2	44.17	30.77	7.48	17.58
	3	47.54	29.84	4.97	17.65
	4	47.50	29.82	6.23	16.45
0.3	1	47.58	28.03	5.65	18.74
	2	47.54	28.85	5.00	18.61
	3	48.87	27.87	6.52	16.74
	4	47.51	27.73	7.12	17.64

shows that the Cr substitution induces a negative pressure in the material. It is worth to mention that a sample with higher Cr concentration,  $x = 0.4$ , was also prepared. However, the presence of secondary phases was observed (see the Supplemental Material for details [23]). The insets of Fig. 1 show SEM images taken for the samples, which reflect homogeneous compositions without presence of secondary phases. EDX analysis was performed at four different locations on each sample, marked in the figure. The element concentration at the four spots, shows a homogeneous distribution through the sample, within the limits of the EDX technique (Table I and Supplemental Material [23]). We note that from EDX results, it seems that the Cr content between sample  $x = 0.2$  and  $x = 0.3$  is quite similar, however, as we will show next, there is a consistent change on the transition temperatures and magnetic properties on the samples that indicates the effect of Cr substitution. As  $x = 0.3$  is a critical composition (for higher Cr values secondary phases appear) it is possible that some disorder is already present in the sample that alters the EDX results but it is just too small to detect. For the results and discussion we will refer to the nominal  $x$  value for simplicity.

Figures 2(a)-2(c) show temperature-dependent magnetization data,  $M(T)$ , for all samples, at 0.01 (right axis), 2, and 6 T (left axis), recorded upon cooling (closed symbols) and subsequent heating (open symbols). All samples undergo a first-order martensitic transition at temperatures  $T_M$  below the ferromagnetic ordering temperature  $T_C$ . The hysteresis width observed around the first-order martensitic transition in these alloys is approximately 10 K or larger. For the alloy with  $x = 0.1$ , the martensitic transition takes place on cooling at  $T_M = 270 \text{ K}$  from a ferromagnetic austenite phase ( $T_C = 312.5 \text{ K}$ ) to a weakly magnetic martensite, that orders ferromagnetically at around 200 K. In this weakly magnetic martensitic both antiferromagnetic and ferromagnetic interactions are present [24]. With Cr substitution, the ferromagnetism of the martensitic phase is enhanced over the antiferromagnetism and the structural transition takes place between two ferromagnetic phases. In the other two alloys,  $x = 0.2$  and  $x = 0.3$ , the martensitic transition takes place between the ferromagnetic austenite and the ferromagnetic martensite state. The substitution of Mn by Cr shifts the martensitic

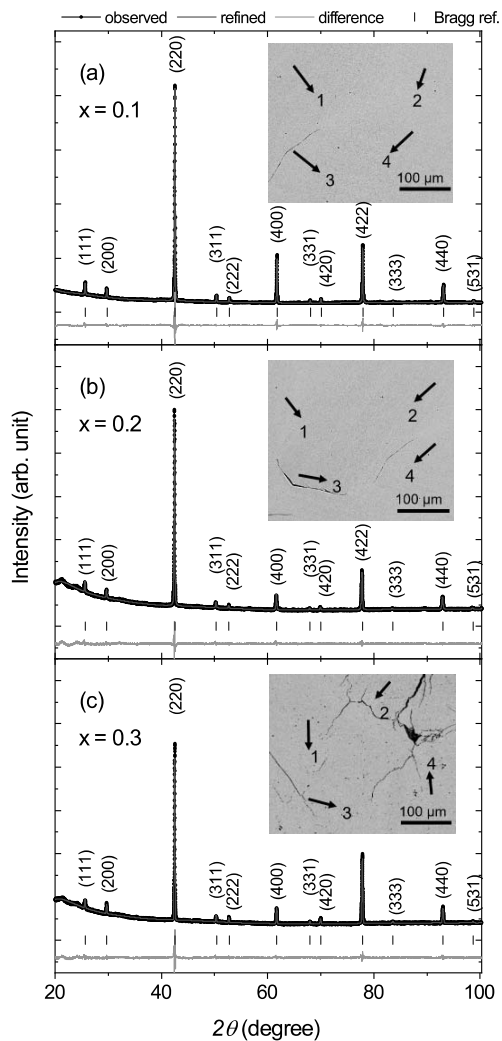


FIG. 1. XRD results of the  $\text{Ni}_2\text{Cr}_x\text{Mn}_{1.4-x}\text{In}_{0.6}$  samples at room temperature, for (a)  $x = 0.1$ , (b)  $x = 0.2$ , and (c)  $x = 0.3$ . Calculated diffractograms and differences to the observed ones are also shown for each sample. The positions of the Bragg peaks are indicated. The inset shows room-temperature SEM images of each alloys. Black arrows indicate the spots where the composition was analyzed in detail.

transition towards lower temperatures and enhances the ferromagnetic interactions in the martensite phase, as also reported for Ni-Mn-Cr-Sb alloys [25]. We have measured the magnetization at 10 K for all samples and the magnetic moment of the martensite phase increases with Cr substitution (see Supplemental Material [23]). Consequently, the magnetization difference between the martensite and austenite phases decreases.

Table II gathers the characteristic transition temperatures of the samples, determined as the inflection points of the  $M(T)$  curves.  $T_C$  is the Curie temperature in the austenite,  $T_M$  is the martensitic transition temperature upon cooling, and  $T_A$  indicates the reverse martensitic transition, upon heating, as it is

marked in Fig. 2(c). Additionally, in Fig. 2(b) we have also marked the austenite start temperature  $A_s$  and the austenite finish temperature  $A_f$ . For all samples,  $T_M$  decreases linearly with field, as shown in the inset of Fig. 2(b) for  $x = 0.2$ . As has been seen in other Ni-Mn-Z-based Heusler alloys (with  $Z = \text{In, Sb, Sn}$ ), the magnetic field shifts the structural transition toward lower temperatures as the austenite phase is stabilized.  $dT_M/dH$  is extracted as the slope of the linear fit of  $T_M$  versus field [inset of Fig. 2(b)] and quantifies the sensitivity of the martensitic transition to the magnetic field. This value for the Cr-doped alloys is rather weak compared with the Ni-Mn-In parent compound ( $dT_M/dH \approx -7 \text{ K/T}$  [8]) but still higher than for other Ni-Mn-based Heusler alloys [26]. According to the Clausius-Clapeyron equation  $dT_M/dH \cong \mu_0 \Delta M / \Delta S$ , the sensitivity of the martensitic transition to the field not only depends on the magnetization jump at the transition  $\Delta M$  but on the transition entropy change  $\Delta S$ . Actually,  $\Delta S$  has a higher influence on  $dT_M/dH$  as  $\Delta M$  [27]. It has been shown as well, that in Ni-Mn-Z ( $Z = \text{In, Sn, Sb}$ ) Heusler alloys the transition entropy strongly depends on the distance between the Curie temperature and the martensitic transition temperature  $|T_C - T_M|$ . The entropy of the transition decreases with the increase of  $|T_C - T_M|$  [28–31]. With Cr substitution in the  $\text{Ni}_2\text{Cr}_x\text{Mn}_{1.4-x}\text{In}_{0.6}$  series, the distance  $|T_C - T_M|$  increases as can be seen in Table II, so it is expected that  $\Delta S$  decreases with Cr. Consequently, a decrease of  $dT_M/dH$  is also observed through the series of samples.

Figures 2(d)-2(f) present magnetic-field-dependent magnetization,  $M(H)$ , up to 6 T for all samples, recorded at selected temperatures around the martensitic transformation. Two measurements were performed at each temperature in order to check the reproducibility of the first-order induced transition. The closed symbols are data measured after reaching the target temperature,  $T_i$ , following the discontinuous heating protocol (DHP) described below and the open symbols shows the data subsequently measured without heating or cooling in between. In the DHP, the sample was first heated up to 350 K (fully austenite phase), followed by cooling down to 200 K (fully martensite phase) and then reaching  $T_i$  upon heating.

We choose the selected temperatures to lie below  $T_A$ , meaning that the sample is in the martensite state, before applying the magnetic field. Therefore, the austenite state is induced due to the magnetic field. Interestingly, different results are obtained for the samples. In the case of  $x = 0.1$ , 6 T is sufficient to induce a complete reverse martensitic transition at the selected temperatures, while for  $x = 0.2$  and  $0.3$  the transition is not complete. However, for the latter compounds the magnetization behavior is more reproducible, i.e., the repeated hysteresis loops lie close to the first ones. In the case of the alloy with  $x = 0.1$ , there is a large difference between the first and the following data for the sweep up branch. When  $T_i$  is reached following the DHP the field-induced transition is quite broad, for instance, at  $T_i = 265 \text{ K}$  the transition starts around 3 T and finishes around 5 T while, for the following cycle, it finishes around 4 T. Additionally, the magnetization does not increase monotonically but shows step-like features. For the down sweep (austenite to martensite transition), both curves follow the same path. These step-like features are re-

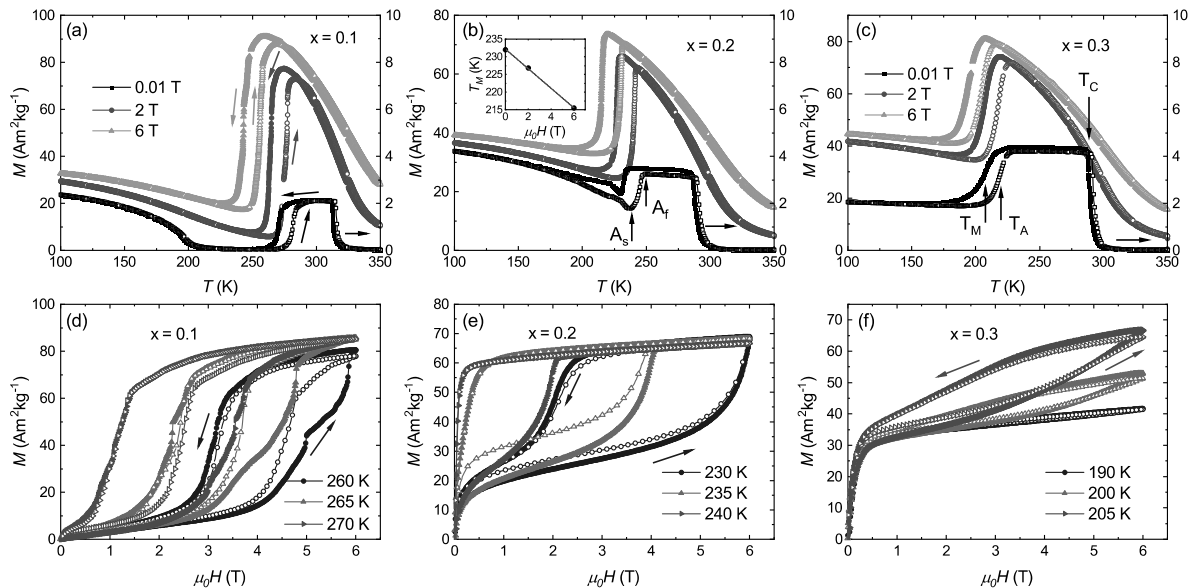


FIG. 2. Temperature dependence of the magnetization of  $\text{Ni}_2\text{Cr}_x\text{Mn}_{1.4-x}\text{In}_{0.6}$  for (a)  $x = 0.1$ , (b)  $x = 0.2$ , and (c)  $x = 0.3$  at magnetic fields of 0.01, 2, and 6 T. The right axes show the scale for the 0.01 T data. Closed symbols indicate measurements upon cooling and open symbols those recorded during heating. The inset of (b) shows the variation of  $T_M$  with field and the red line is the linear fit to the data. Field-dependent magnetization at different temperatures for (d)  $x = 0.1$ , (e)  $x = 0.2$ , and (f)  $x = 0.3$ . Closed symbols indicate first measurement after reaching the target temperature following the discontinuous heating protocol (see text) and open symbols indicate repeated measurements without heating or cooling in between.

TABLE II. Transition temperatures of the  $\text{Ni}_2\text{Cr}_x\text{Mn}_{1.4-x}\text{In}_{0.6}$  alloys. For the definition of  $T_C$ ,  $T_A$ ,  $T_M$  see Fig. 2(c).

$x$	$T_C$ (K)	$T_M$ (K)	$T_A$ (K)	$dT_M/dH$ (K/T)
0.1	312.5	270	281.5	-4.6
0.2	288	232	245	-2.8
0.3	288.5	207.8	219.8	-2.5

lated to the way the austenite phase grows into the martensite phase, or, in other words, the annihilation of the martensite [32] and it is observed every time  $T_i$  is reached following the DHP.

From the  $M(H)$  curves it is also possible to see that the martensite state of the alloys with  $x = 0.2$  and  $x = 0.3$  is ferromagnetic at temperatures close to  $T_A$ .

We have measured the adiabatic temperature change  $\Delta T_{ad}$  during magnetic field pulses of 2 and 6 T. First pulses were obtained following the DHP and follow-up pulses, without heating or cooling in between, were applied at selected temperatures. First, we will discuss the results for 6 T pulses.

Figure 3 shows time-dependent data of  $\Delta T_{ad}$  at selected temperatures, together with the time-dependent magnetic field. At temperatures  $T_i$  above  $T_A$ , close to  $T_C$ , when the samples show a conventional MCE,  $\Delta T_{ad}$  follows closely the applied magnetic field change with only little delay (less than 1 ms) due to experimental artifacts (black curve in Fig. 3). For lower  $T_i$ , however, when the inverse MCE appears,  $\Delta T_{ad}$  follows the field change only with large delay and strongly

disturbed time-dependent profiles. Specifically, for the case of  $x = 0.1$ ,  $T_i = 265$  K [blue curve in Fig. 3(a)] lies below the austenite start temperature,  $A_s = 275$  K, and, as it can be seen in the  $M(H)$  curves showed in Fig. 2(d), at this temperature the transition from martensite to austenite is induced and completed (i.e. the sample transforms back when the field is reduced). When the measurement is repeated [light blue curve in Fig. 3(a)], without heating or cooling the sample in between, a similar result is obtained, however smaller effects are observed. This is reflected as well on the magnetization data. The  $M(H)$  curves in Figs. 2(d)-2(f) can help to understand the  $\Delta T_{ad}$  results, but no one-to-one comparison should be made, as the pulse-fields measurements are performed under adiabatic conditions while the static-field  $M(H)$  are done under isothermal conditions [33].

At  $T_i = 275$  K and  $x = 0.1$  [red in Fig. 3(a)], the MCE is highly irreversible due to the fact of being in the middle of the hysteresis region. After the pulse, a large fraction of the sample remains in the austenite and does not transform back to the martensite phase. When a second pulse is given [dark red in Fig. 3(a)], the result is a mixture of inverse MCE, due to the transformation from martensite to austenite and conventional MCE caused by the austenite already present in the sample after the first pulse. A similar behavior is observed for the other two samples. The results in blue are for a  $T_i < A_s$  and red ones are for  $A_s < T_i < A_f$ , where  $A_f$  is the austenite finish temperature (see Fig. 2(b)). It is worth to point out that, while there is a large difference of the  $M(H)$  results for the different samples [Fig. 2(d)-2(f)] the  $\Delta T_{ad}$  results appear quite similar